RECENT RESEARCH ON MAGNETOSPHERIC WAVE-PARTICLE INTERACTIONS

R. A. HELLIWELL, U. S. INAN, J. P. KATSUFRAKIS, D. L. CARPENTER and E. W. PASCHAL

Space, Telecommunications, and Radioscience Laboratory, Stanford University, California 94305, U.S.A.

Abstract: Highlights of recent Stanford University VLF research in the Antarctic include new observations of wave-induced particle precipitation and controlled experiments on nonlinear wave growth phenomena. Higher-than-expected levels of burst precipitation have been discovered inside the plasmasphere, near $L=2$, using subionospheric signal perturbations called "Trimpi events". Studies of burst precipitation have been extended to the region poleward of the plasmapause using the Siple transmitter signal as a waveguide probe. Experiments on the "coherent wave instability", using the amplitude and frequency modulation capability of the new Siple transmitter, have produced exciting new results. Examples are: 1) better definition of the power threshold for the stimulation of temporal wave growth, 2) generation of strong sidebands by unamplified "beat" waves and 3) generation of chorus-like elements within a band of simulated hiss. Using a new digital processing technique developed at Stanford, new features of the phase behavior of growing waves have been found. Opportunities for extending these experiments are discussed.

1. Introduction

New experiments on wave-particle interactions in the magnetosphere performed by Stanford University have produced interesting, and in some cases, suprising results. Highlights of this work are reviewed briefly in the following sections: (i) observations of wave induced particle precipitation, (ii) experiments on wave instabilities using the Siple VLF transmitter, (iii) digital processing of Siple transmitter signals. In the final section, future plans and opportunities for extending these experiments are discussed.

2. Observations of Wave Induced Particle Precipitation

Significant progress has recently been made in the use of perturbations in the amplitude and phase of subionospherically propagating signals ("Trimpi events") to indicate the occurrence of wave induced burst precipitation into the lower ionosphere. Research has been concentrated in two main areas, one involving precipitation effects within the plasmasphere, the other effects induced near to and poleward of the plasmapause.

2.1. Precipitation effects equatorward of the plasmapause

This precipitation research has been concentrated at Palmer Station (65°S, 64°W,

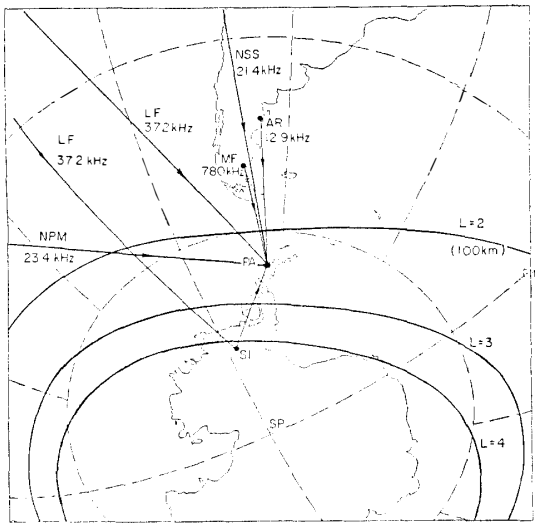

Fig. 1. Map showing great circle paths from a number of signal sources to Palmer, Antarctica (PA).

$L \sim 2.4$), with supporting measurements at Siple (76°S, 84°W, $L \sim 4.3$). Figure 1 shows a map of the Palmer and Siple vicinity; great circle paths from a number of VLF/LF/MF signal sources are indicated. Figure 2 shows a Palmer chart recording of simultaneous perturbations on five of these sources. Following is a brief summary of recent findings.

1) Most observed signal perturbations are time-correlated with the receptionof a whistler (HELLIWELL *et al.*, 1973; CARPENTER and LABELLE, 1982). The correlation is often one to one; at other times only some subset of the observed whistlers is associated with amplitude perturbations. In one case study the subset of correlated whistlers was found to be unique, in that they propagated on a particular magnetospheric path that was not followed by the uncorrelated events, but which was favorably located (as determined from arrival bearing measurements) for purposes of inducing amplitude perturbations at the receiver (CARPENTER and LABELLE, 1982).

2) Typical signal changes on paths 2000–10000 km in length are $\sim$1–2 db in amplitude and $\sim$1 microsecond in phase delay, developing within $\sim$1 s and decaying over periods of $\sim$10–100 s (HELLIWELL *et al.*, 1973; LOHREY and KAISER, 1979). The development time is related to the combined effects of the duration and propagation time of the whistler and the travel times to the ionosphere of the pitch-angle scattered electrons following their interactions with the wave. The decay time is believed to be governed by the attachment rate of electrons to neutrals at the $\sim$85 km nighttime reflection altitude for VLF (DINGLE, 1977).

3) The amplitude perturbations are most easily recognized in analog records under conditions of darkness at $\sim$100 km altitude. In the daytime the corresponding precipitation undoubtedly occurs, since magnetospheric wave activity is high at such times, but its existence tends to be masked by the effects of solar radiation. Trimpi events are usually detected at the relatively high signal levels that are characteristic of darkness over the entire propagation path, but they can be recognized at much lower signal levels, for example when a long sea path is sunlit from the source to a

point ~2000 km from the receiver (LEYSER *et al.*, 1984).

4) The observations have extended from VLF to LF and MF frequencies. The occurrence rate on a 37.2 kHz LF signal at Palmer was found to be comparable to the rates on the most active VLF channels (CARPENTER *et al.*, 1984). Figure 2, fourth panel, shows an example of this activity. The MF perturbations on a ~1800 km path to Palmer (map of Fig. 1) occurred on nights of high activity on VLF paths, but fewer than 10 MF events were usually detected as compared to >50 on the active VLF paths. The MF perturbations were of order 50% in amplitude and were not in general followed by a ~30 s decay toward a pre-event level, as is usually the case for the VLF signals.

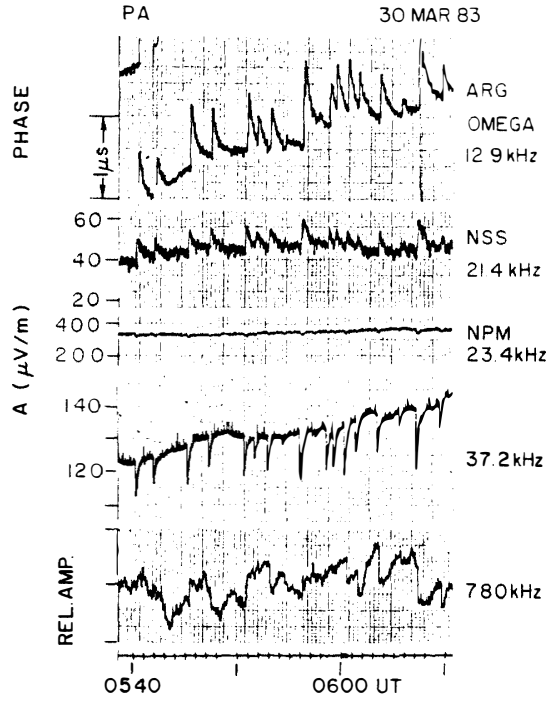

Fig. 2. Observation of simultaneous perturbations on five subionospheric signals received at Palmer Station, ranging in frequency from 12.9 to 78.0 kHz (from CARPENTER et al., 1984).

5) In a recent study of Palmer data for the period March 3 to April 7, 1983, events were detected on NSS, 37.2 kHz, and NPM on 70% of the nights (LEYSER *et al.*, 1984). Typical occurrence rates on nights of prolonged activity were near 10/hr. Detection of 20 to 30 events/hr was not unusual, and during peak activity over 50 events/hr were observed.

6) Trimpi-event activity observed at Antarctic stations appears to maximize at the equinoxes (CARPENTER and LABELLE, 1982). In the austral summer, conditions of darkness along the signal paths are either not realized or are seldom realized near Antarctic stations. In the austral winter, other types of relatively fast signal variations may tend to mask Trimpi events. However, the winter decrease appears to be a real effect.

7) Trimpi events have been found to occur preferentially during, and for days following, major magnetic storms (CARPENTER and LABELLE, 1982). A supporting

but less well defined relation to magnetic activity was found in a recent study of Palmer data by LEYSER *et al.* (1984).

8) During a March–April, 1983 observing period at Palmer, there was a high day-to-day correlation in activity levels on the NSS, 37.2 kHz and NPM signals. There was also a tendency for the majority of events to occur simultaneously on more than one signal (LEYSER *et al.*, 1984).

9) The perturbations on a given signal at a particular station are usually of one sign, positive on NSS (at Palmer), and negative on 37.2 kHz and NPM (see examples in Fig. 2). However, periods both of mixed signs and of the opposite sign are observed (LEYSER *et al.*, 1984).

10) In one case study, the individual whistler component correlated with perturbations on NSS at Palmer was identified as noted in 1) above (CARPENTER and LABELLE, 1982). Above a field strength of 13 μV/m, the amplitude of this component was found to be linearly related to the NSS perturbation amplitude, while for cases of less than 13 μV/m, no NSS change was detected.

11) The first direct evidence of precipitating electron bursts associated with lightning has been obtained from the SEEP satellite experiments (VOSS *et al.*, 1984). A one to one correlation was found between relativistic electron precipitation bursts measured by a sensitive detector on the S81-1 polar orbiting satellite and observations at Palmer of broad band whistlers that originated in the northern hemisphere and were associated with Trimpi events. The satellite precipitation data showed evidence of particle echoing between conjugate hemispheres. The satellite was located in the northern hemisphere at a distance of approximately 2000 km from the Palmer meridian, thus suggesting that a single lightning flash can precipitate electrons at two widely spaced locations.

2.2 Analysis and interpretation

Particles scattered by a magnetospheric wave propagating on a field aligned path would be expected to precipitate in a region near the ionospheric exit point of the scattering wave and its conjugate. Thus by triangulating on the wave exit point, it should be possible to estimate the location of the precipitation. CARPENTER and LABELLE (1982) used a combination of occurrence data on amplitude perturbations and information on whistler arrival bearing and path equatorial radius to infer that perturbed ionospheric regions affecting NSS at Palmer were located within a region extending $\sim$400 km equatorward of the station and also within $\sim$200 km of the affected great circle paths, but not necessarily overlapping them. The individual precipitation regions were estimated to be of order 100 km in the east-west direction.

Another means of locating precipitation regions is to combine information on sunrise-sunset terminator position with occurrence information on multiple paths. Using this method, and in particular the NPM path to Palmer, LEYSER *et al.* (1984) concluded that most of the relevant precipitation regions were located within $\sim$1000 km of Palmer. However, perturbations in distant regions were also indicated; some events observed after sunrise over Palmer suggested that the precipitation regions were in dark areas as far as $\sim$1800 km away.

The occurrence data suggest that there is a belt of relatively high Trimpi activity

near Palmer, extending from $L=2$ to $L=3$. Using a test particle model of the whistler-particle interaction, CHANG and INAN (1985) studied the energy spectra and temporal profile of whistler-induced precipitation fluxes within the plasmasphere. Their results indicate that for the higher energy electron precipitation ($E>40$ keV) required for penetration to the 80–90-km VLF reflection altitudes, there exists an inner magnetospheric region ($2<L<3$) where the level of whistler induced precipitation can be expected to be comparatively high.

Palmer data show clearly that significant precipitation is produced in the southern hemisphere at times of whistlers that originate in the north. This implies that a large fraction of the precipitating particles first travel northward after undergoing a counter-streaming interaction with the whistler. They then mirror back, without precipitating, due to the high mirror altitudes in the north, and travel southward where precipitation occurs.

The test particle model has been used to study various aspects of this situation. Figure 3 shows the computed precipitation flux induced by a single whistler component

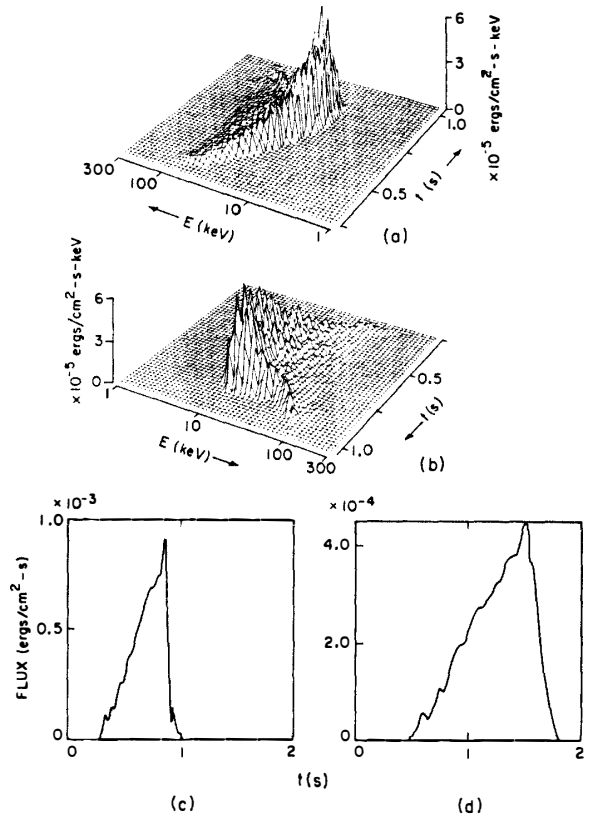

Fig. 3. Computed precipitation flux induced by a single whistler component originating in the northern hemisphere and propagating on the $L=3$ field line. (a) Northern hemisphere precipitated flux as a function of energy and time. (b) Same result shown from a different perspective. (c) Northern hemisphere (direct) precipitation flux versus time obtained by integrating (a) over energy. (d) Precipitated flux that would be observed in the southern hemisphere, resulting from pitch angle scattered particles that first travel to the north and then, due to the asymmetry of the earth's magnetic field near the South Atlantic anomaly, mirror at relatively high altitude and precipitate in the south (adapted from CHANG and INAN, 1985).

generated by a lightning impulse in the northern hemisphere and propagating on the $L=3$ field line (see CHANG and INAN (1985) for additional details). Figures 3a and 3b show the dynamic energy spectrum (presented as a 3-dimensional display of flux versus time and energy as seen from two different perspectives) of the whistler-induced precipitation flux that would be observed in the northern hemisphere, where the lightning discharge that launches the whistler wave is assumed to occur at $t=0$. The time of equatorial crossing of the whistler wave front at 8.0 kHz is indicated by an arrow. As the whistler wave moves toward the magnetic equator, it begins to interact with and scatter particles of relatively high energy that subsequently arrive at the ionosphere earlier than do lower energy particles that interact nearer to the equatorial plane (INAN *et al.*, 1982). Once past the equator, the wave again interacts with higher energy particles at high southern latitudes, and these particles arrive at the ionosphere approximately at the same time as the lower energy particles that have resonated with the wave earlier. This "arrival time convergence" effect accounts for the accumulation of the flux near $t \approx 0.8$ s. Figure 3b shows that at even later times the flux consists only of higher energy particles that have interacted with the wave at latitudes even further south.

Figure 3c shows the temporal profile of the whistler-induced flux obtained by integrating the result of Fig. 3a over all energies. The time of onset, risetime and duration of this "precipitation pulse" can be compared to observed precipitation signatures (for example in terms of Trimpi events) in order to extract information about the wave-induced precipitation process in the magnetosphere. Figure 3d shows the "mirrored precipitation" flux that would be observed in the southern hemisphere. This involves the same particles that constitute the energy flux of Fig. 3c; they mirror in the northern hemisphere (due to the asymmetry of the mirror heights near the South Atlantic anomaly) and precipitate in the south. The increased dispersion of the pulse is due to travel time differences between particles at various energies.

2.3. *Precipitation effects poleward of the plasmapause*

In the region equatorward of the plasmapause, the Trimpi effect provides the only ground-based method found so far that can detect burst precipitation induced by magnetospherically propagating whistler-mode waves. However, in the region poleward of the plasmapause, such precipitation has been observed by a variety of instruments (*e.g.* ROSENBERG *et al.*, 1971; HELLIWELL *et al.*, 1980; ARNOLDY *et al.*, 1982). It seems clear that the Trimpi effect can provide a powerful means of supporting and substantially extending these measurements because of the large size of the regions probed by the subionospheric signals. A problem then is to find suitable signal sources and observing locations.

In early work, bursts of noise propagating just outside the plasmapause were found to produce amplitude perturbations on a long path to Siple Station ($L \sim 4.3$) and on a 600 km path from NAA to the northern hemisphere conjugate station, Roberval, Canada (DINGLE and CARPENTER, 1981). The bursts, lasting about 10 s, occurred every few minutes and were triggered by whistlers. A remarkable feature of this case is an overshoot or prolonged 2–5 min recovery effect. It was suggested that the Trimpi events were interrupting a pre-existing drizzle precipitation, and that several

minutes were then required before the drizzle flux could be re-established.

Significant progress in middle to high latitude studies has been achieved through a recent series of experiments involving subionospheric VLF signals from Siple Antarctica received at several Antarctic locations. Figure 4 shows a map of these stations and the relations of the signal paths to L values at 100 km altitude.

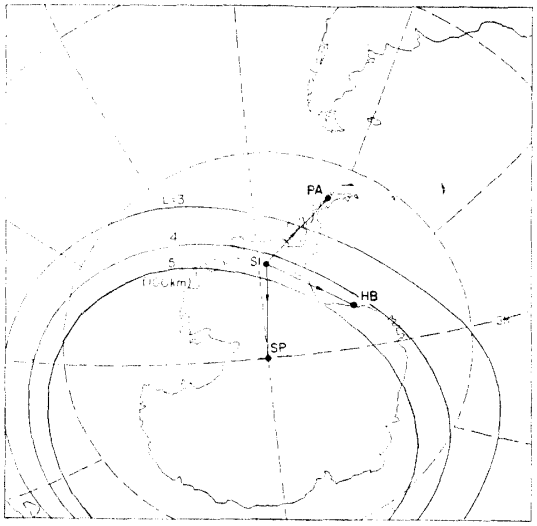

Fig. 4. Map showing subionospheric signal paths from the VLF transmitter at Siple Station (SI) to Palmer (PA), Halley (HB), and South Pole (SP).

In one case study, simultaneous burst precipitation events were observed on a 3.79 kHz Siple signal received at Halley and at South Pole (CARPENTER *et al.*, 1985). Figure 5 shows an example of the South Pole data from this period. The upper two panels display amplitude and phase, respectively, with amplitude referred to 10 μV/m. Two events are shown, characterized by amplitude decreases of $\sim$2 db and phase advances of $\sim$15 μs. Similar events were observed at Halley Station.

Figure 5c shows a longer segment of the phase data; it is compared on panel d to a spectrogram of correlated whistler and VLF emission events (marked by vertical lines in the upper margin).

The phase and amplitude records of Fig. 5 were produced by digital analysis of the original broadband tape recordings. A pilot tone recorded with the tape data is used as a reference for correcting the digital data for tape speed variations (PASCHAL and HELLIWELL, 1984).

Fast phase advances on the Siple signal have also been observed at Palmer Station (CARPENTER *et al.*, 1985). In one case, analysis of the correlated whistlers showed that the precipitation was occurring just inside the plasmapause at $L \sim 3.2$, at a distance at least 700 km from the receiving station.

Continuing study of Siple signals received at Halley shows extensive evidence of burst precipitation effects (A. J. SMITH, personal communication, 1984). It appears that when outside the plasmapause, such a path at nearly constant L is exposed to effects induced by a wide variety of wave events, including whistler triggered chorus and various types of emission bursts.

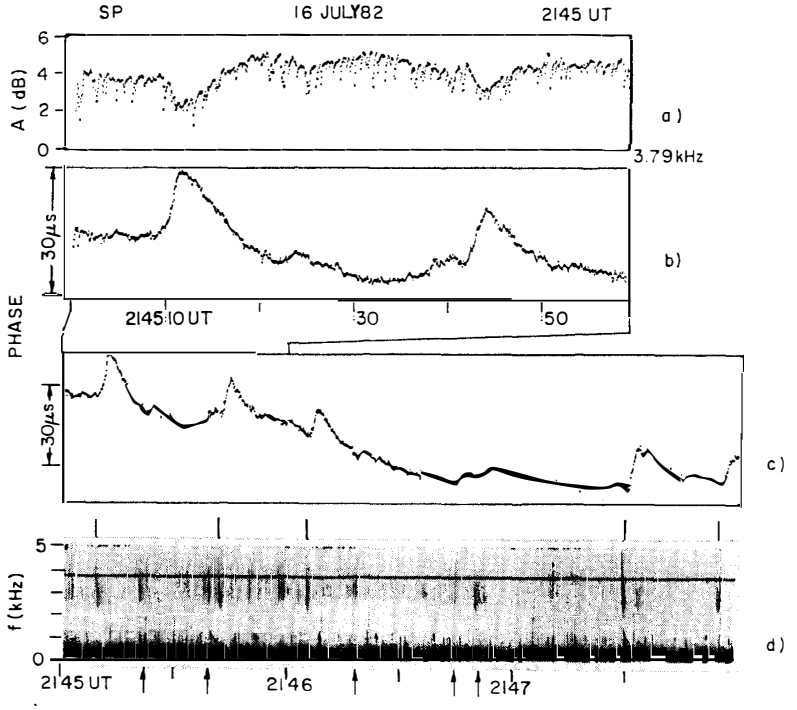

Fig. 5. South Pole data showing fast wave-induced perturbations on a subionospheric 3.79 kHz signal from the Siple transmitter. (a) Digital analysis of signal amplitude. (b) Digital analysis of Siple signal phase. (c) Additional phase data shown on a compressed time scale. (d) Broadband spectrogram associated with the time period of (c) (from CARPENTER et al., 1985). See text for additional details.

3. Experiments on Wave Instabilities Using the Siple VLF Transmitter

Using the new VLF transmitter (Jupiter) installed at Siple station in 1979, it is possible to radiate a variety of wave forms with precise control of frequency, phase and amplitude. For example, it is now possible to simultaneously introduce two independent coherent waves on different frequencies. This flexibility has led to exciting new experiments, several of which are described in the following paragraphs.

3.1. Threshold experiments

In earlier work, a power threshold was found for the stimulation of temporal growth of coherent waves (HELLIWELL *et al.*, 1980). When the threshold is crossed, total growth increases, usually by 20 db or more. An explanation of this threshold for development of what is called the "coherent wave instability" or CWI has not yet been found, and its continued study is a major part of recent and projected future Siple activity.

With the Jupiter transmitter the time required to perform the threshold experiment has been dramatically reduced, from ~ 30 s to 1 s. The reason is that the amplitude of Siple pulses can now be changed rapidly (once every millisecond). Thus the threshold can be observed on a time scale that is much shorter than the characteristic time (~ 10 s) for temporal changes in the particle flux to occur (STILES and

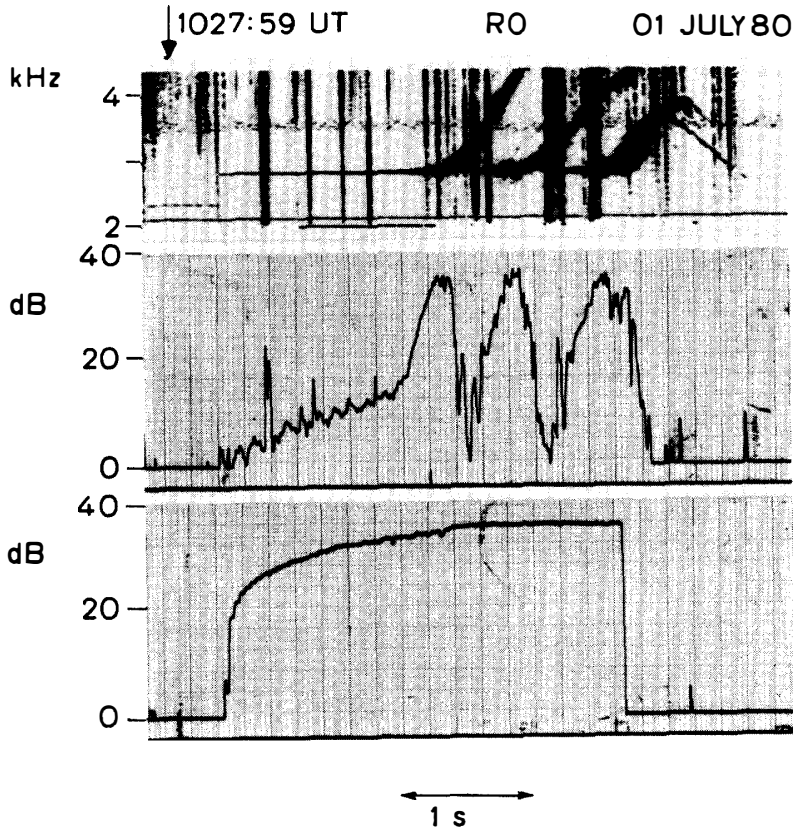

Fig. 6. Roberval, Canada records showing the threshold effect as part of the magnetospheric response to the injection of a variable-amplitude 3-s pulse at 2.83 kHz from the Siple, Antarctica VLF transmitter. Top panel: dynamic spectrum of the received pulse. Middle panel: relative received signal intensity in a 100-Hz bandwidth centered on the carrier. Lower panel: relative amplitude in db of the transmitted pulse.

HELLIWELL, 1977). An example of the new threshold experiments is shown in Fig. 6. The amplitude of an injected 3 s pulse is increased with time over a range of 30 db, as shown in the lower panel. The dynamic spectrum of the signal and its associated triggered emissions as observed at Roberval are shown in the upper panel. The middle panel shows the intensity level of the received signal in db versus time, as measured in a 100 Hz bandwidth filter centered on the carrier. The key feature is the sudden change in growth rate occurring at the threshold, located at + 16 db on the output curve. At this point the input signal is only 2–3 db below its maximum value. At the threshold the apparent growth rate changes from ~10 to 80 db/s. Since at this point the input signal rises at ~2.5 db/s, the pre-threshold output growth rate is actually 7.5 db/s. Following saturation four rising emissions are triggered. As can be seen from the figure, all of the stimulated wave energy is carried away by each rising emission, leaving the input signal at its original or even lower amplitude. After each emission the carrier regrows to the same saturation level at approximately the same rate (80 db/s) and then triggers another similar emission. Available data show that the saturation level is not simply related to the growth rate. Current models of coherent wave growth do not adequately explain saturation.

In a recently published paper (HELLIWELL and INAN, 1982), a feedback model of the CWI is used to interpret the observations. An interaction region, several hundred wavelengths long, is centered on the magnetic equator (for constant frequency). It is treated like a feedback amplifer with a delay line and an open loop gain of G. For $G>1$ the system is unstable and can generate self-excited oscillations. In this case the temporal growth rate is given by $\gamma=(G-1)/T$, where T=effective loop delay. Saturation is reached when G falls to unity. The effective value of G is determined by the phase-bunching process which may be a function of the applied field and the background noise level. At this point it is not known exactly what controls the value of G. One possibility is that the threshold is related to the distribution of the interacting particles. An understanding of the threshold could lead to new diagnostic techniques for monitoring particle fluxes from the ground.

3.2. Multi-frequency experiments

As new frequency components are added to an injected signal, the total signal begins to acquire the characteristics of broad-band noise. Thus the investigation of multi-frequency excitation is a critical element in bridging the gap between the classical Kennel-Petschek (1966) theory and the coherent wave instability.

In a recent experiment, two coherent VLF waves closely spaced in frequency were transmitted simultaneously. Both their frequency separation and their relative amplitudes were varied in various ways with time. In one format, shown in Fig. 7, the input signals were of equal strength and their frequency difference Δf was varied linearly with time from 5 to 45 Hz. At 20 Hz the steady state output reached a minimum that was as much as 15–20 db below the saturation level of either wave by itself. This result agrees with earlier amplitude and frequency modulation experiments which

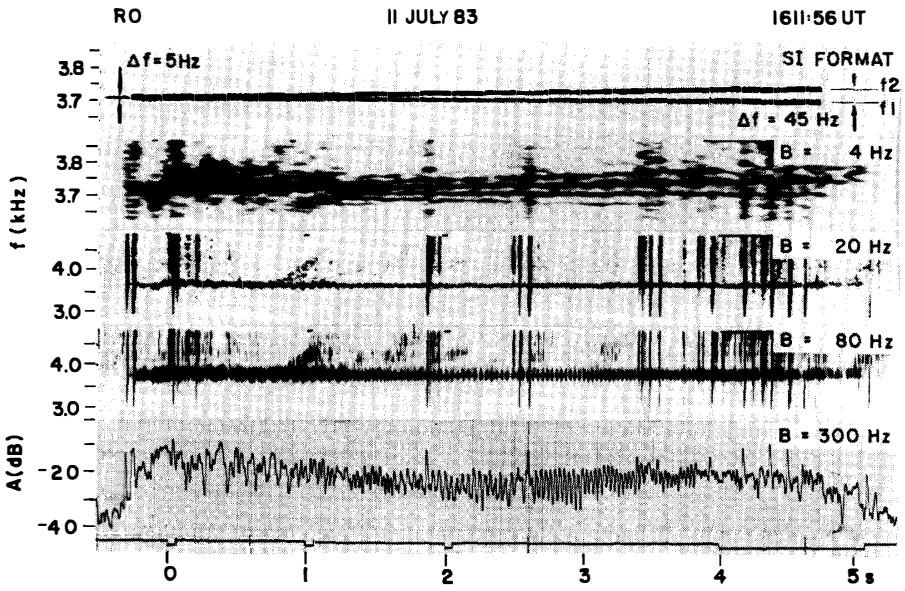

Fig. 7. A two-frequency Siple transmitting experiment in which the frequency difference between two signals of equal strength was varied linearly with time from 5 to 45 Hz, as shown in the top panel. The received spectra, analyzed with varying filter bandwidths, are shown on the next three panels. The bottom panel shows the received amplitude in a 300 Hz band.

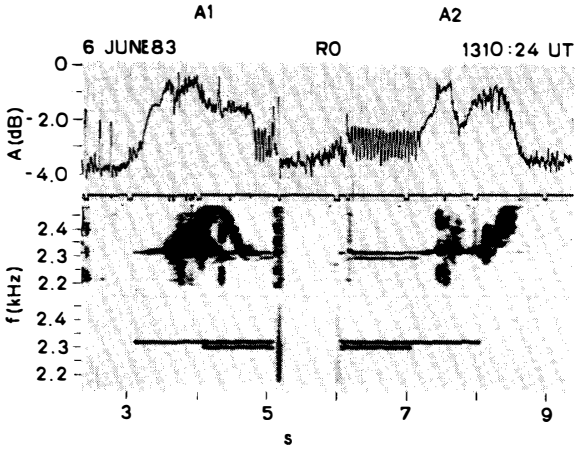

Fig. 8. A two-frequency Siple transmitting experiment in which the frequency separation was held constant at 20 Hz and the lower-frequency signal was turned off at the beginning or end of a two-second sequence. The transmitted format is shown in the bottom panel, and the received spectra and associated amplitude are shown above.

showed minimum output at a modulation frequency of 20 Hz. In the next experiment, illustrated in Fig. 8, Δf was held constant at 20 Hz and both input signals were applied with equal amplitude for 1 s. When either the upper or lower component was turned off, the remaining component switched immediately to the normal single frequency growth rate. In the reverse experiment the second signal was turned on after the first had reached saturation and was triggering. The suppression developed in less than about .25 s, a time much shorter than the many seconds delay in suppression observed in the so-called "quiet-band" experiment (RAGHURAM *et al.*, 1977). These new results many require a revision in the currently accepted explanation of the quiet band (CORNILLEAU-WEHRLIN and GENDRIN, 1979).

In addition to suppression of growth, the two-frequency experiments show that sidebands are frequently generated at frequencies spaced by Δf. Sidebands up to order 7 have been observed. Of particular interest is the fact that the sideband amplitude tends to maximize at a particular ratio of the input intensities of the two signals and at a particular Δf. Strong sidebands are seen from Δf's of 10 Hz up to perhaps 70 Hz or more, with signal intensity ratios of the order of 15 db producing the maximum sideband output. These results can be explained qualitatively by a combination of enhanced wave-growth at the frequency of the stronger input wave and modulation of this stimulated emission at the beat frequency. However, strong sidebands are generated even when the input waves themselves show little or no temporal growth. This result appears to disagree with most current theories of sideband generation, which are based on electron trapping by waves that are much stronger than the predicted unamplified signals from Siple Station.

3.3. Noise simulation experiments

Noise simulation experiments have been devised to explore the relations between diffuse noise phenomena such as mid-latitude hiss and discrete emissions of the chorus type. A natural hiss band was simulated with repeated one-second sequences of 10 ms pulses as illustrated in Fig. 9. The frequency of each pulse was chosen randomly from a set of uniformly spaced frequencies in a 400 Hz frequency band. The phase of the transmitted wave was continuous at each step in frequency. Following one-hop propagation to Roberval the visual appearance of the dynamic spectrum resembled

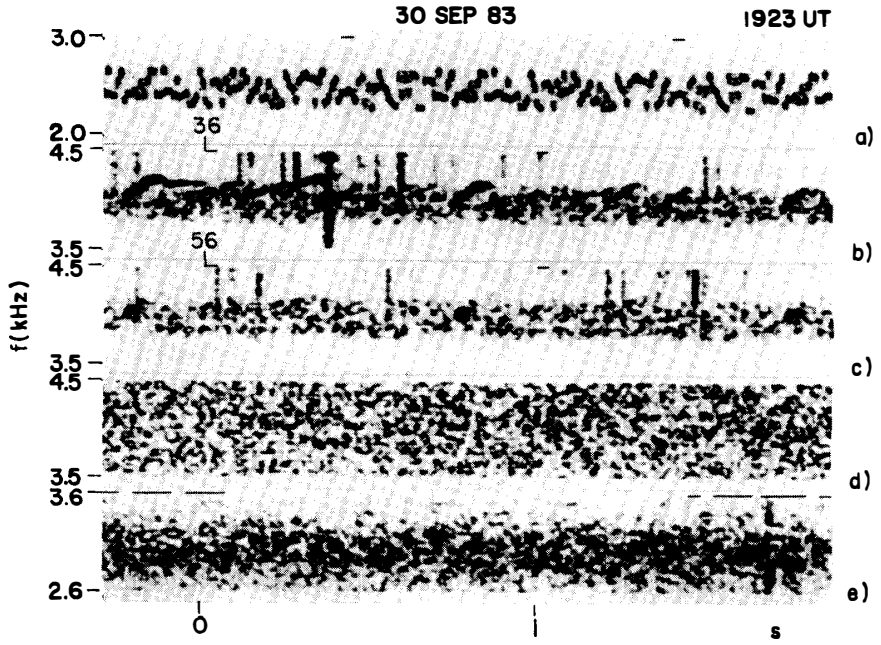

Fig. 9. Noise simulation experiment. (a) Spectrum of the transmitted signal, consisting of 10-ms pulses randomly distributed in frequency within a 400 Hz band, but repeated in the same order each second. (b) Received spectrum at Roberval, showing development of discrete emissions at points within the received band. (c) Received signal 30 s later, with only limited evidence of discrete emissions. (d) Spectrum of broadband noise simulated in the laboratory. (e) A natural magnetospheric hiss band.

that of random noise. The noise envelope showed fluctuations in amplitude that were attributed to phase mixing between pulses on different frequencies, resulting from dispersion over the signal path. At certain times in the format, the simulated hiss showed chorus-like elements that would appear repeatedly at the same location in each pulse train. However, over several tens of seconds these elements would change in shape or disappear entirely to be replaced by others at different locations in the 1 s period. This effect is tentatively attributed to a tendency for the 10 ms wave trains to link together to form extended quasi-coherent elements. The phases of several individual 10 ms pulses that comprise the chorus element happen to be such as to resonate with a single electron, giving rise to enhanced growth. As time passes the relative phasing changes, causing other combinations of pulses to appear as chorus elements. These results suggest that hiss and chorus may have a common origin. Further experiments will be aimed at developing this connection.

4. Digital Processing of Siple Transmitter Signals

Because of the narrowband character of the observed growth and emissions, it is important to know how the phase of the output signal varies with time. A new digital technique has been developed (PASCHAL and HELLIWELL, 1984) for flexible processing of the phase of the received signal. With the aid of a stable pilot tone recorded on the original analog magnetic tapes, it is possible to remove all tape flutter and reproduce the relative phase of the received signal. An example of this technique as applied

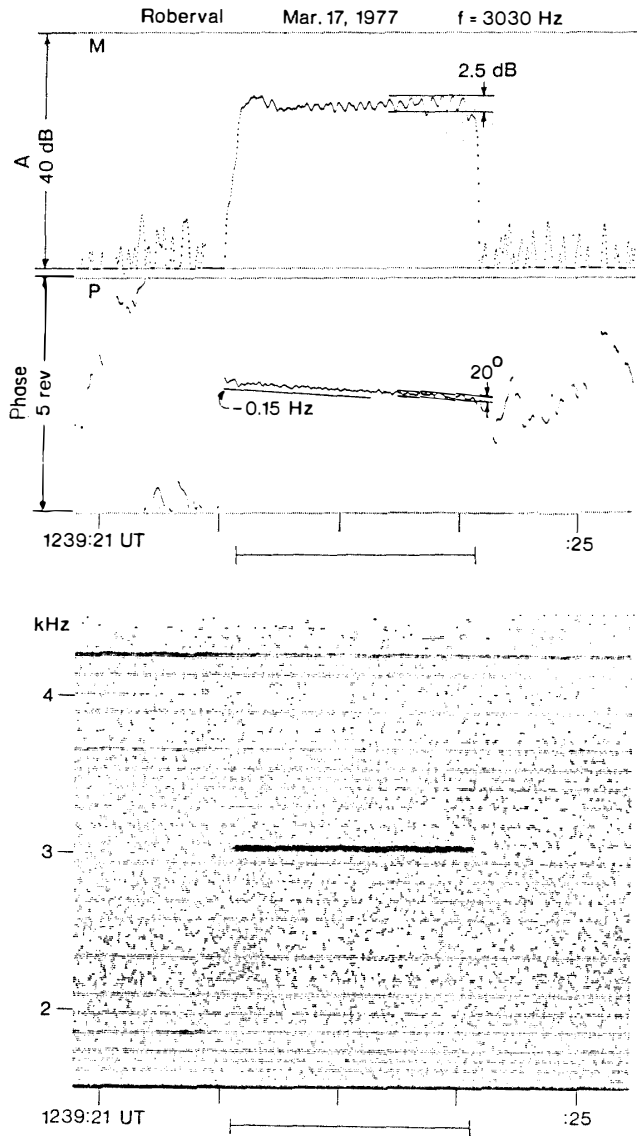

Fig. 10. Application of a new digital processing technique to an unamplified, nontriggering 2-s pulse from the Siple transmitter, received at Roberval. A digital spectrogram is shown below. Above are displayed the amplitude and phase behavior of the received signal.

to an unamplified non-triggering pulse is shown in Fig. 10. The total signal does not vary more than 2.5 db over the 2 s duration of the pulse while the phase slowly decreases with time. The corresponding frequency change is -0.15 Hz, typical of the frequency shifts caused by cross-L drift of the magnetospheric duct through which the signal propagates. Although the spectrum and the amplitude trace show little evidence of growth, there is a curious periodic fluctuation in amplitude with a frequency of ~ 11 Hz. It is postulated that this pulsation results somehow from the phase-bunching of particles, where the average G in the feedback model is <1 and hence there is no unstable growth.

More interesting is the case where temporal growth and triggering are observed, as shown in Fig. 11. Here the amplitude is observed to increase at the rate of about

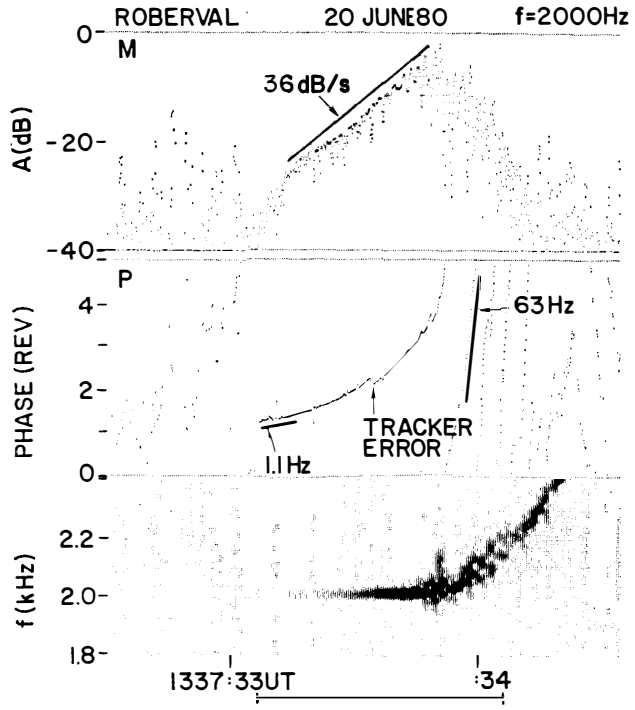

Fig. 11. Application of a new digital processing technique to a Siple pulse on which temporal growth and triggering were observed. A spectrogram of the signal is shown below. Above are the amplitude and phase analyses.

36 db/s, while the phase increases monotonically with time. The phase trace is approximately parabolic, indicating a linear increase in frequency with time. In all cases of growth examined so far, the phase is observed to advance with time. The only negative phase changes (of more than brief duration) are those connected with non-amplifying pulses of the type shown in Fig. 10. The discontinuity in the slope of the pulse trace at the time of triggering (~ 0.7 s after start of pulse) may be related to the so-called "triggering window" (HELLIWELL and INAN, 1982), a transient condition where the stimulated radiation, through a progressive phase shift, cancels the input signal at a certain point in time and space. However, current models (NUNN, 1974; DOWDEN *et al.*, 1978; HELLIWELL and INAN, 1982) do not adequately account for the observations.

5. Future Plans and Opportunities

5.1. Burst precipitation observations

In the area of burst precipitation observations, or studies of the Trimpi effect, there are three major areas of opportunity. One is at middle latitudes, where studies are needed of the spatial structure and distribution of wave induced events. Much has been learned about the occurrence of Trimpi effects, but only limited knowledge has been obtained about key questions such as the number and distribution of the regions excited by a single whistler, the effective area of a perturbed region, the position of the region with respect to the affected great circle signal paths, the correlation of the activity with specific types of lightning activity in the conjugate region, the effects

of ducted as opposed to nonducted magnetospheric signals, and the existence of threshold and saturation effects in the process.

A second area of opportunity is the remote "imaging" of precipitation by means of multichannel subionospheric signal monitoring at individual high latitude sites. By observing signals with a range of arrival bearings at a given location, information can be obtained on the "azimuth" of precipitation activity. The location information can then be refined through the kinds of "triangulation" available from similar observations at other stations, through DF on associated wave activity, and through wave dispersion analysis. This work will help to extend the spatial range of precipitation studies now being done within more restricted ionospheric viewing areas.

A third area of opportunity is world-wide study, based upon observations of approximately north-south signal paths at coastal stations encircling the Antarctic. The distribution of stations in longitude on the Antarctic coast affords a unique opportunity to answer questions regarding the worldwide distribution of burst precipitation activity. Such questions concern the degree of longitudinal uniformity in the activity, its dependence upon worldwide thunderstorm activity and its relation to the South Atlantic magnetic anomaly.

5.2. VLF transmitting experiments

Plans are being made to increase the VLF effective radiated power at Siple Station through the use of a circularly-polarized antenna. Provision will be made to vary the injected wave polarization. Both near term and long range plans are motivated by recent experimental findings. One of the most significant of these provided an answer to a key question: can measurable precipitation be induced through controlled VLF transmissions? This was answered affirmatively in the recent SEEP satellite experiments aboard polar orbiting satellite S81-1 (IMHOF *et al.*, 1983). The principal requirement for reaching the necessary levels of detection is adequate transmitter power. *In situ* wave observations on the DE 1 and ISEE satellites, in which the signal levels from Siple and from the Omega systems have been compared, suggest that an injected wave power of 10–20 kW is needed from Siple in order to achieve the conditions of nonlinear wave growth that are required for further controlled studies of the coherent wave instability and associated precipitation effects.

With higher radiated power, realized in large part through a phased antenna array, it will be possible to investigate aspects of the coherent wave instability that have only been partially explored, such as saturation and the effects of diminished wave coherence on output wave levels.

Acknowledgments

We are grateful for the support of our colleagues at Stanford and for the excellent work of our field engineers. This research was supported by grants from the Division of Polar Programs of the National Science Foundation for work at Siple, Roberval, Palmer and South Pole. Additional support in specific areas was provided by NASA.

References

ARNOLDY, R. L., DRAGOON, K., CAHILL, L. J., Jr., MENDE, S. B. and ROSENBERG, T. J. (1982): Detailed

correlations of magnetic field and riometer observations at $L=4.2$ with pulsating aurora. J. Geophys. Res., **87**, 10449–10456.

CARPENTER, D. L. and LABELLE, J. W. (1982): A study of whistlers correlated with bursts of electron precipitation near $L=2$. J. Geophys. Res., **87**, 4427–4434.

CARPENTER, D. L., INAN, U. S., TRIMPI, M. L., HELLIWELL, R. A. and KATSUFRAKIS, J. P. (1984): Perturbations of subionospheric LF and MF signals due to whistler-induced electron precipitation bursts. J. Geophys. Res., **89**, 9857–9862.

CARPENTER, D. L., INAN, U. S., PASCHAL, E. W. and SMITH, A. J. (1985): A new VLF method for studying burst precipitation near the plasmapause. J. Geophys. Res., **90**, 4383–4388.

CHANG, H. C. and INAN, U. S. (1985): Lightning-induced electron precipitation from the magnetosphere. J. Geophys. Res., **90**, 1531–1541.

CORNILLEAU-WEHRLIN, N. and GENDRIN, R. (1979): VLF transmitter-induced quiet bands; A quantitative interpretation. J. Geophys. Res., **84**, 882–890.

DINGLE, B. (1977): Burst precipitation of energetic electrons from the magnetosphere. Ph. D. thesis, Stanford Univ., Stanford, Calif.

DINGLE, B. and CARPENTER, D. L. (1981): Electron precipitation induced by VLF noise bursts at the plasmapause and detected at conjugate ground stations. J. Geophys. Res., **86**, 4597–4606.

DOWDEN, R. L., MCKAY, A. D., AMON, L. E. S., KOONS, H. C. and DAZEY, M. H. (1978): Linear and nonlinear amplification in the magnetosphere during a 6.6-kHz transmission. J. Geophys. Res., **83**, 169–181.

HELLIWELL, R. A. and INAN, U. S. (1982): VLF wave growth and discrete emission triggering in the magnetosphere; A feedback model. J. Geophys. Res., **87**, 3537–3550.

HELLIWELL, R. A., KATSUFRAKIS, J. P. and TRIMPI, M. L. (1973): Whistler-induced amplitude perturbation in VLF propagation. J. Geophys. Res., **78**, 4679–4688.

HELLIWELL, R. A., CARPENTER, D. L. and MILLER, T. R. (1980): Power threshold for growth of coherent VLF signals in the magnetosphere. J. Geophys. Res., **85**, 3360–3366.

IMHOF, W. L., REAGAN, J. B., VOSS, H. D., GAINES, E. E., DATLOWE, D. W., MOBILIA, J., HELLIWELL, R. A., INAN, U. S., KATSUFRAKIS, J. and JOINER, R. G. (1983): Direct observation of radiation belt electrons precipitated by the controlled injection of VLF signals from a ground-based transmitter. Geophys. Res. Lett., **10**, 361–364.

INAN, U. S., BELL, T. F. and CHANG, H. C. (1982): Particle precipitation induced by short-duration VLF waves in the magnetosphere. J. Geophys. Res., **87**, 6243–6264.

LEYSER, T. B., INAN, U. S., CARPENTER, D. L. and TRIMPI, M. L. (1984): Diurnal variation of burst precipitation effects on subionospheric VLF/LF signal propagation near $L=2$. J. Geophys. Res., **89**, 9139–9143.

LOHREY, B. and KAISER, A. B. (1979): Whistler-induced anomalies in VLF propagation. J. Geophys. Res., **84**, 5122–5130.

NUNN, D. (1974): A self-consistent theory of triggered VLF emissions. Planet. Space Sci., **22**, 349–378.

PASCHAL, E. W. and HELLIWELL, R. A. (1984): Phase measurements of whistler mode signals from the Siple VLF transmitter. J. Geophys. Res., **89**, 1667–1674.

RAGHURAM, R., BELL, T. F., HELLIWELL, R. A. and KATSUFRAKIS, J. P. (1977): A quiet band produced by VLF transmitter signals in the magnetosphere. Geophys. Res. Lett., **4**, 199–202.

ROSENBERG, T. J., HELLIWELL, R. A. and KATSUFRAKIS, J. P. (1971): Electron precipitation associated with discrete very-low-frequency emissions. J. Geophys. Res., **76**, 8445–8452.

STILES, G. S. and HELLIWELL, R. A. (1977): Stimulated growth of coherent VLF waves in the magnetosphere. J. Geophys. Res., **82**, 523–530.

VOSS, H. D., IMHOF, W. L., WALT, M., MOBILIA, J., GAINES, E. E., REAGAN, J. B., INAN, U. S., HELLIWELL, R. A., CARPENTER, D. L., KATSUFRAKIS, J. P. and CHANG, H. C. (1984): Lightning-induced electron precipitation. Nature, **312**, 740–742.

(*Received February 20, 1985*)